

Thermoreflectance CCD Imaging of Self Heating in AlGa_N/Ga_N High Electron Mobility Power Transistors at High Drain Voltage

Kerry Maize

Department of Electrical Engineering
University of California, Santa Cruz
Santa Cruz, CA, USA
kerry@soe.ucsc.edu

Eric Heller and Donald Dorsey

Materials and Manufacturing Directorate
Air Force Research Laboratory
Wright-Patterson Air Force Base OH, USA, 45433-7707

Ali Shakouri

Birck Nanotechnology Center
Purdue University
West Lafayette, IN, USA 47907-2057
shakouri@purdue.edu

Abstract—Thermoreflectance CCD imaging with sub-micron spatial resolution was used to characterize self heating nonuniformity in two finger AlGa_N/Ga_N high electron mobility power transistors at equivalent power (1.27 W) for different combinations of drain and gate voltage. Thermoreflectance images of device surface temperature revealed formation and redistribution of local hotspots as transistor drain voltage increased from $V_D=10.7$ V to 50 V. For all bias points, heating between the two fingers was not fully uniform. At high drain voltage, heating migrated toward the drain side of the channel and increased thermal nonuniformity was observed along symmetric drain and source fingers. Direct microthermocouple measurements confirmed spatial temperature nonuniformity observed in thermoreflectance images. Results demonstrate the usefulness of fast thermoreflectance imaging to inspect self heating in Ga_N thin film power devices with high spatial resolution.

Keywords-component; Thermoreflectance imaging; Ga_N; HEMT; Power Transistors; Self Heating

I. INTRODUCTION

There is increasing demand for integrated microelectronic power devices that can operate at extremes of frequency, power, and temperature. To extend beyond the limitations of silicon based power electronics, engineers are exploring novel materials such as gallium nitride (Ga_N) for integrated power transistors. Ga_N has several material properties that make it advantageous in power electronics. Of primary significance is the ability to engineer modulation doped AlGa_N/Ga_N interfaces with very high electron mobilities. These films can be incorporated in high electron mobility transistors (HEMT). Other significant material advantages of Ga_N are its large bandgap of 3.4 eV, which permits high breakdown voltage due to a much higher electric field at which impact ionization becomes a limiting factor, and much lower intrinsic carrier

concentrations allowing a maximum operating temperature of up to 970 K. [1]

Thermal processes, however, remain a significant factor in performance and reliability of Ga_N based transistor devices. Ga_N HEMTs have shown saturation current dependence on temperature [2]. Due to the high power levels reachable in Ga_N HEMTs and the high electric fields achievable that can force this power to be dissipated in a small volume, temperature gradients can be extreme [3]. Temperature stress affects many degradation phenomena observed in Ga_N power devices such as current collapse during fast switching [3] and pit formation [4,5]. For these reasons self heating in Ga_N devices remains an active area of study, and robust and versatile thermal characterization methods are needed. While Raman thermometry is a scanning laser method that has been used to measure both temperature and stress in Ga_N heterostructures at specific points near the surface and with some limited spatial resolution below the Ga_N surface [3,6], one method that is particularly well suited to measure heating across the entire surface of microelectronic devices is thermoreflectance CCD imaging [7-9]. Thermoreflectance imaging measures reflected visible wavelength illumination to provide two dimension maps of surface temperature distribution with submicron spatial resolution and 50 mK temperature resolution. The superior spatial resolution allows thermal imaging of Ga_N device features on a scale much smaller than is possible using infrared imaging. This paper presents results of thermoreflectance CCD images of a Ga_N HEMT under pulsed operation at various stages of transistor pinch-off for equivalent power. Drain voltage was varied between $V_D=10.7$ V to 50 V with gate voltage adjusted to maintain the same total device power of approximately 1.27 W. In extreme pinch-off with drain voltage above 47.5 V, thermoreflectance images of the active Ga_N HEMT revealed formation of local hotspots along the ohmic metallization and Ga_N channel and general temperature redistribution across the transistor. This redistribution at high

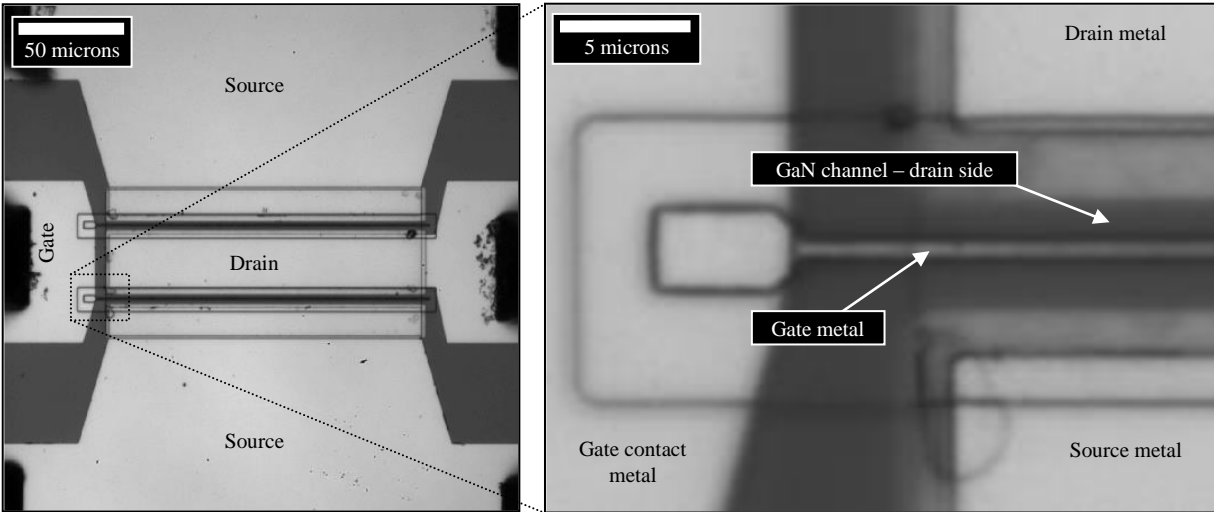


Figure 1. Optical image of two channel AlGaIn/GaN high electron mobility power transistor. The gate width is 150 μm .

drain voltage was also confirmed using direct thermocouple measurements of the active area of the GaN transistor.

A. Device Description

The device was an AlGaIn/GaN high electron mobility transistor (HEMT) consisting of two $\sim 5\ \mu\text{m}$ long by 150 μm wide channels (two fingers) designed for power RF applications. The unpackaged sample was grown on a $\sim 500\ \mu\text{m}$ SiC wafer, and contacted with Cascade Microtech ACP40-L coplanar probes to allow low Ohmic loss and fast RF switching, as shown in Fig. 1. Each finger of the transistor (Fig. 1 inset) was contacted at top and bottom by a grounded source metal and biased drain metal with the active channel (SiN passivated AlGaIn/GaN stack) in between.

With no bias applied to the gate (a Schottky diode contact), the AlGaIn/GaN interface forms a $\sim 2\ \text{nm}$ thin highly conductive layer. This layer is often referred to as a two-dimensional electron gas (2-DEG). Negative gate voltage reverse biases the diode and depletes the conducting layer of carriers by electrostatic field effect and turns the transistor off. As such, this is often the site of a lot of power dissipation, especially when the transistor is only partially turned on. Drain current for the HEMT in this study was negligible for $V_G < -4\ \text{V}$.

II. METHOD

A. Thermoreflectance Imaging

Fig. 2 shows a diagram of the thermoreflectance CCD imaging setup used to acquire thermal images of the active GaN HEMT. The top surface of the HEMT sample is illuminated under a reflectance microscope using a narrow-band LED light source. The light reflected from the sample material surface is recorded on a variable frame rate, 12-bit scientific grade Dalsa CCD camera with 1024x1024 pixel resolution. Camera operation and device excitation timing is controlled by a LabVIEW program and custom designed

hardware trigger board. Repeated device excitation pulses are sent to the HEMT and synchronized to the camera acquisition. For this study, square voltage pulses one millisecond in duration were applied to the drain of the GaN HEMT at 1% duty cycle. For each excitation cycle, the electrical pulse causes a temperature rise in the HEMT, which in turn induces a change in the optical reflectance of the HEMT material surfaces. Images of the HEMT surface reflectance during both the excited (on) and unexcited (off) states are recorded in the CCD camera. Comparing the change in reflectance amplitude for these two images produces a two-dimension thermoreflectance map across the HEMT surface. Thermoreflectance image maps are then converted to temperature maps by applying a thermoreflectance coefficient

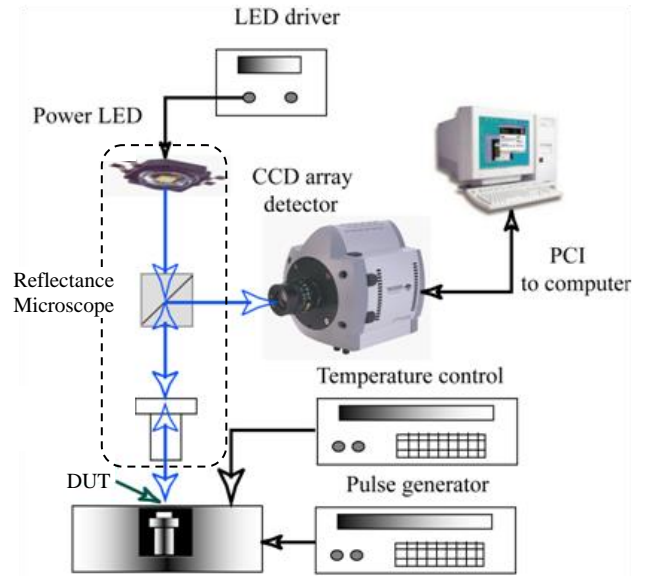


Figure 2. Thermoreflectance CCD imaging and device pulsing configuration.

TABLE I. HEMT BIAS POINTS FOR THERMOREFLECTANCE IMAGES

V_G (V)	V_D (V)	I_D (mA)	Power (W)
2	10.7	119	1.27
-1.43	18.1	70.8	1.28
-2.56	30	41.8	1.25
-3.05	40.1	31	1.24
-3.08	42.5	29.8	1.27
-3.12	45.2	28.5	1.29
-3.17	47.5	26.8	1.27
-3.41	50	25.5	1.28

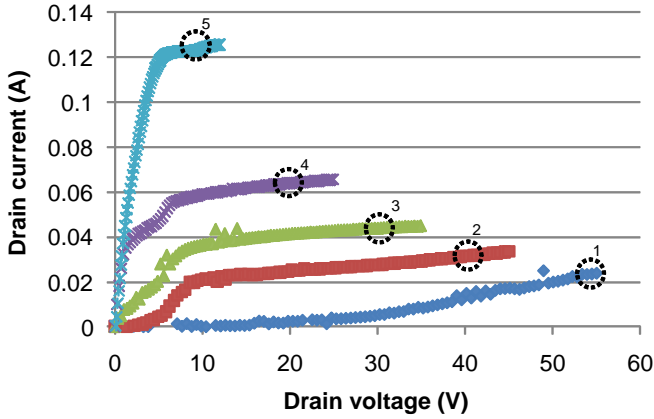


Figure 3. GaN HEMT steady state drain current versus drain voltage for several different gate voltages. The indicated points correspond to equivalent power of 1.27W.

(C_{TH}), which describes a material's quantitative change in optical reflectivity in response to a change in temperature. The thermoreflectance change for most materials is very small, on the order of $10^{-4} C^{-1}$. However, by averaging over many device excitation cycles the thermoreflectance amplitude signal to noise ratio can be sufficient to yield temperature resolution down to 50mK. Averaging times for each thermal image depend on the specific material C_{TH} and desired signal to noise. Most semiconductor and metal materials yield good thermoreflectance images in less than one minute for temperature changes of 1C or greater. For the GaN HEMTs in this study, good signal to noise was obtained for the ohmic contact metal regions in about thirty seconds. However, each image was averaged for 30 minutes to improve signal to noise on the GaN, which has a smaller C_{TH} than the metal .

Experimental calibration of the GaN HEMT material C_{TH} is performed in a procedure separate from device thermal imaging. Calibration involves heating the entire sample uniformly using an external micro-thermoelectric stage. The temperature induced change in optical reflectance over the entire sample is recorded by the CCD while temperature is measured simultaneously using a type E microthermocouple. C_{TH} for each material region of interest on the sample are

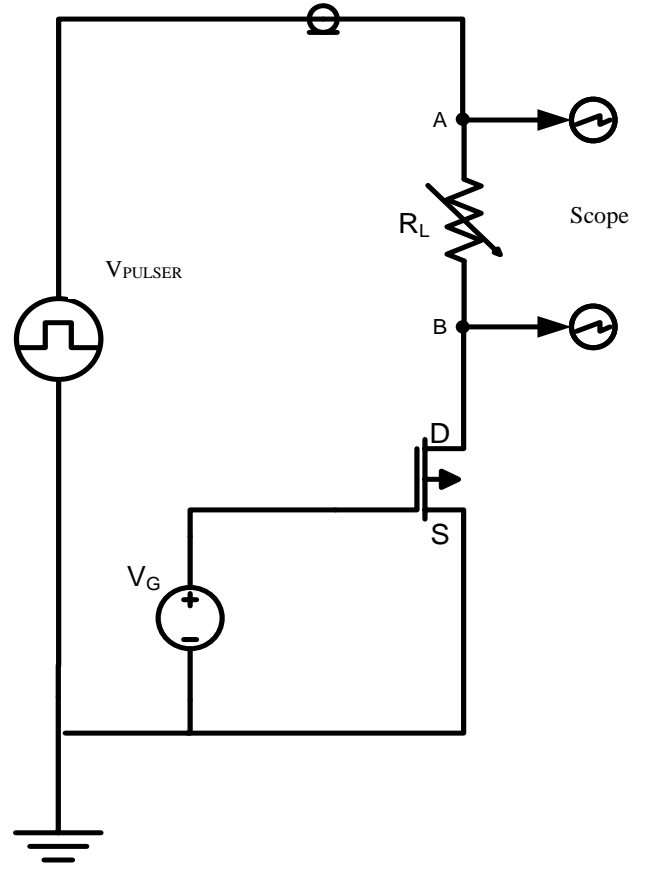


Figure 4. Thermoreflectance pulsing circuit for the GaN HEMT.

obtained by comparing the calibration image and thermocouple measurements. C_{TH} depends on the wavelength of external illumination [9], and a green 530 nm LED was found to be a good choice for the HEMT sample due to its relatively high C_{TH} on the drain and source metal. For a 50X magnification microscope objective with 0.35 numerical aperture, experimental calibration yielded a C_{TH} on the surface metal (Fig. 1 “Drain”, “Source”, “Gate contact” metals) of $2.6 \times 10^{-4} C^{-1}$. Calibration of C_{TH} for GaN using the LED wavelengths available for this study did not yield results consistent with separate direct thermocouple temperature measurements of the active HEMT device. Consequently, thermoreflectance results for the GaN regions of the HEMT are presented in arbitrary units.

B. Device Pulsing Parameters

Self heating in the HEMT was studied for different combinations of drain voltage and current at equivalent power. Fig. 3 shows the GaN HEMT steady state drain current versus drain voltage curves for several different gate voltages. The steady state measurements were obtained using an HP 4156B parametric analyzer, with the device probed on wafer. The highlighted bias points show different combinations of drain voltage and drain current all corresponding to the same 1.27 W power dissipation, but some open channel and some mostly closed. Thermoreflectance CCD images were obtained for the

bias points in Table 1 to compare HEMT surface spatial temperature distribution at the various stages of pinch-off.

Fig. 4 shows the thermoreflectance pulsing circuit. For each bias point during thermoreflectance imaging drain voltage was pulsed while gate voltage was held constant to maintain the transistor at a specific level of pinch-off. Thermal images were averaged for 30 minutes per image. Drain voltage was applied using a Berkeley Nucleonics (BNC) 202H high voltage pulser. The specified rise time for the pulser is 3 ns rising edge and 10ns falling edge. Drain current was measured from the voltage drop across a variable resistor placed in series with the device. The variable resistor was set to 50 ohms while measuring the highest drain currents (71 and 119 mA) and to 500 ohms to improve accuracy while measuring the lower currents in pinch-

off (25-41 mA). Drain voltages reported represent the potential drop from drain to source across the transistor, and do not include the voltage drop across the resistor R_L . The drain voltage pulse waveform was monitored during thermoreflectance image acquisition to ensure correct bias of the HEMT.

Studies have revealed that GaN based transistors can experience both permanent and temporary performance degradation after extended electrical stress due to formation of trapping states. Because acquisition of a single thermoreflectance image can require averaging over thousands of HEMT excitation cycles, it was important to quantify any device degradation during imaging. Device integrity was measured by comparing the HEMT steady state drain IV before

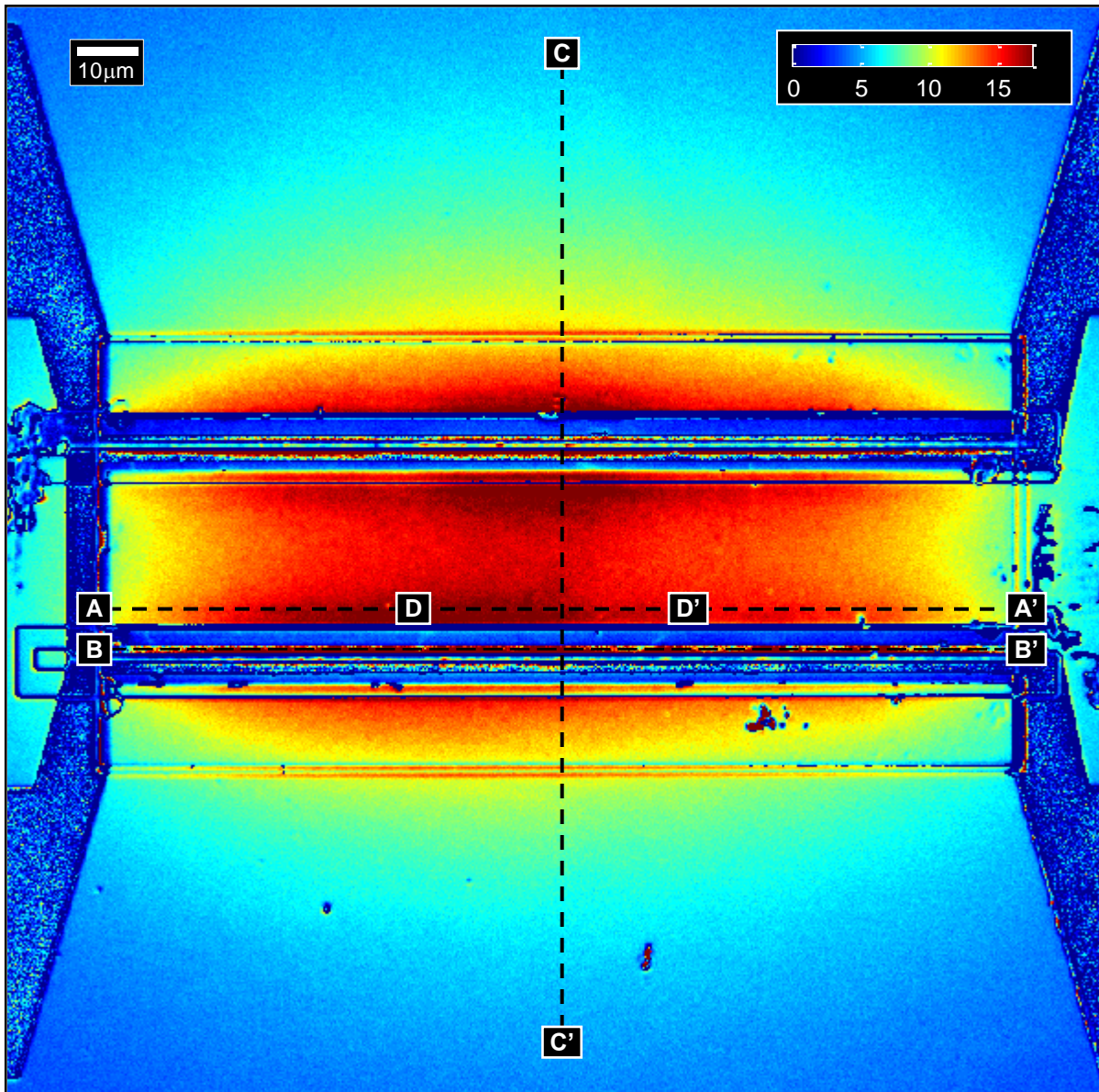


Figure 5. Thermoreflectance image of the GaN HEMT for the bias point $V_D = 50$ V, $I_D = 25$ mA, and $V_G = -3.41$ V. Location of profile lines are indicated.

and after each thermoreflectance image was obtained. These checks revealed less than 2% change in HEMT IV performance due to imaging electrical stress, which is within the noise threshold of the DC measurement apparatus.

III. RESULTS

Analysis of thermoreflectance images of the active GaN HEMTs revealed a redistribution of spatial surface temperature for the cases of extreme transistor pinch-off ($V_D = 47\text{ V}, 50\text{ V}$.) Experiment results demonstrating hotspot dependence on drain voltage are presented in the following section. Spatial temperature distribution is analyzed using both thermoreflectance data calibrated for temperature on the contact metal, and uncalibrated thermoreflectance amplitude profiles for the GaN material regions. Heating distribution is analyzed along both a horizontal and a vertical dimension of the HEMT, revealing hotspot dependence on drain voltage for profiles both parallel to and perpendicular to the gate width. Results of direct microthermocouple measurements are also

presented showing local HEMT temperature increase at high V_D (extreme transistor pinch-off.)

A. Temperature Profiles Parallel to The Gate Width

Fig. 5 shows the thermoreflectance image of the GaN HEMT for the single bias point of $V_D = 50\text{ V}$ and $I_D = 25\text{ mA}$. Gate voltage is -3.4 V . Fig. 6 plots the calibrated horizontal temperature profiles measured on the drain contact metal near the lower of the two HEMT fingers for the full range of drain voltages $V_D = 10.7\text{--}50\text{ V}$ at equivalent power (1.27 W .) The location of the measured profiles is indicated by line A-A' in the thermal image of Fig. 5. The profiles are taken parallel to the gate width. Two temperature trends are noticeable in these profiles. First, the average temperature of the drain contact metal profiles increases with drain voltage. This is expected behavior in field effect transistors, with the strongest electric field, and therefore greatest power density, concentrated on the drain side of the transistor channel. Second, temperature becomes redistributed nonuniformly along the horizontal

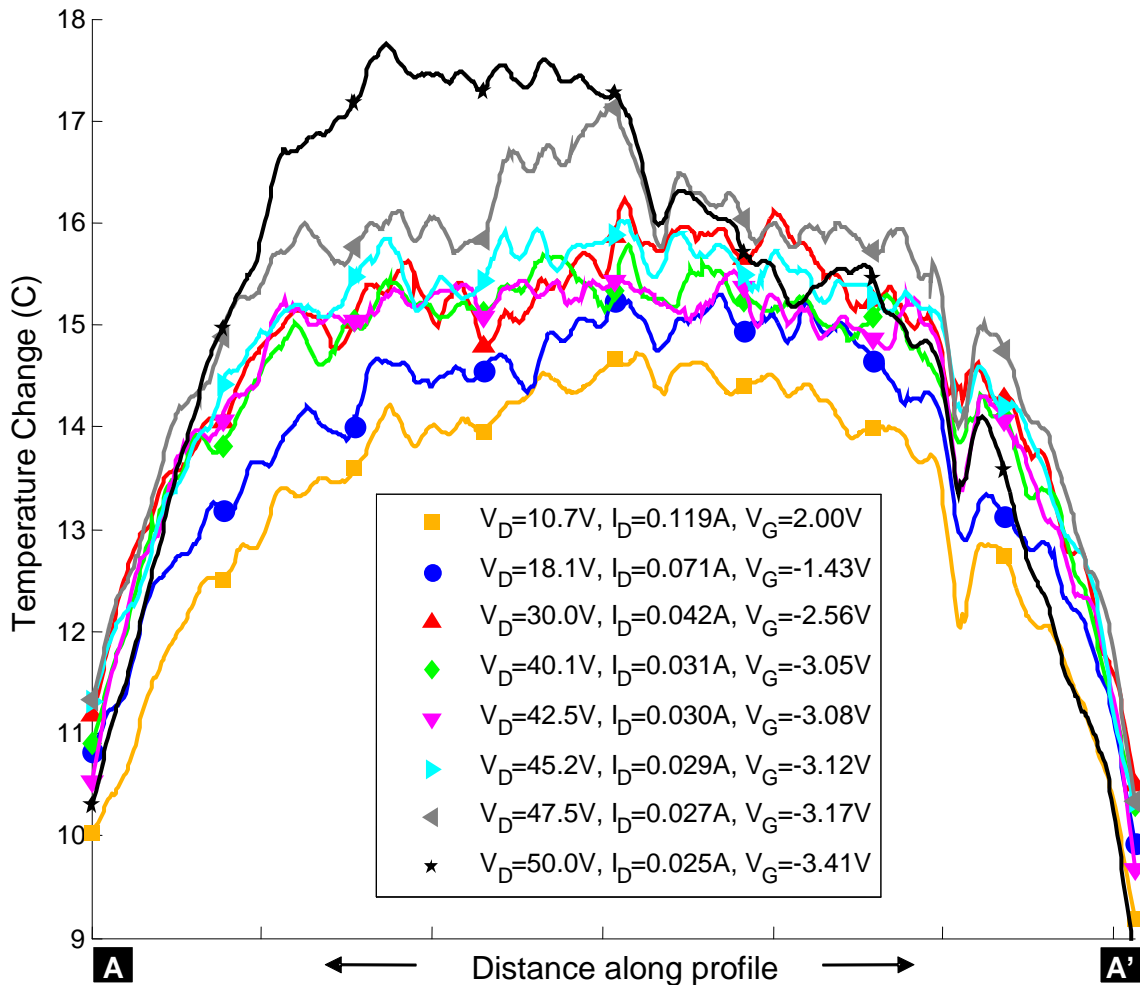


Figure 6. Calibrated horizontal temperature profiles (A-A') measured on the drain metal near the lower of the two channels for the full range of drain voltages $V_D = 10.7\text{--}50\text{ V}$ at equivalent power (1.27 W .)

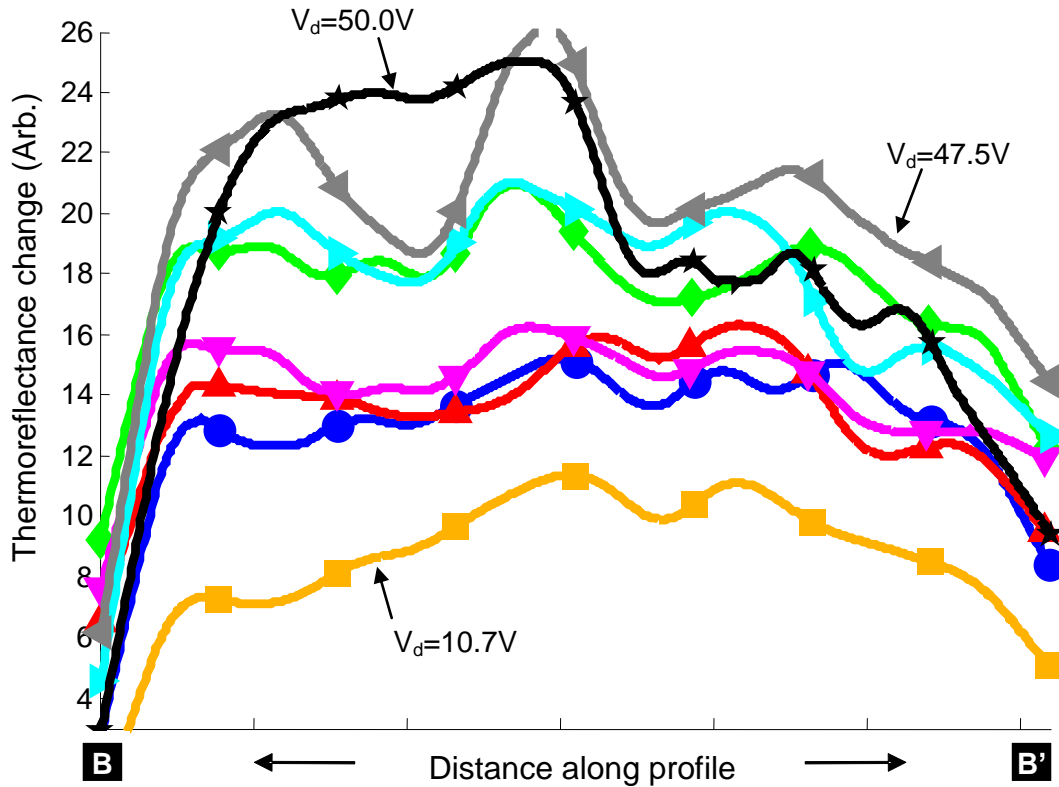


Figure 7. Thermoreflectance change profiles for the gallium nitride material along the channel (profile B-B'). The gallium nitride profiles are not calibrated for temperature.

profile at extreme pinch-off. The profiles corresponding to lower drain voltage ($V_D = 10 \text{ V} - 45.2 \text{ V}$) show an overall symmetric temperature distribution, hotter at the center of the device and cooler at the edges. No abrupt hotspots are visible. At higher drain voltage, $V_D = 47.5 \text{ V}$, $V_G = -3.17 \text{ V}$, a local hotspot first appears near the center of the horizontal profile. The hotspot is seven percent ($1.3 \text{ }^\circ\text{C}$) hotter than the adjoining region of the profile. Temperature nonuniformity becomes more apparent for the next increase in pinch-off bias at $V_D = 50 \text{ V}$, $V_G = 3.41 \text{ V}$. This distribution shows a clear temperature “hump” on the left side of the horizontal profile, as much as 12 percent ($2.1 \text{ }^\circ\text{C}$) hotter than the similar region for the profile at next lower pinch-off bias point of $V_D = 47.5 \text{ V}$. Furthermore, for the highest drain voltage ($V_D = 50 \text{ V}$) the increase in temperature on the left side of the drain finger coincides with a decrease in temperature on the right side of the finger. The average temperature on the right side of the profile at $V_D = 50 \text{ V}$ is four percent lower than the average temperature for the same region at $V_D = 47.5 \text{ V}$. One possible cause of temperature redistribution at extreme pinch-off may be device processing defects that are noticeable only at high drain voltage. These thermal defects are visible due to the high spatial resolution of the thermoreflectance method. Such detail may have appeared blurred under infrared thermal microscopy.

1) Heating in GaN Channel

Horizontal profiles of the GaN surface thermoreflectance amplitude were obtained for the lower finger channel. Profile line B-B' from Fig. 5 was taken on the GaN channel. (See Fig. 1 for enlarged optical images of the nitride channel and gate regions.) The profiles were taken on the drain side of the gate metal. Both the metal profiles and the GaN profiles were obtained from the same series of thermoreflectance images. Fig. 7 plots the thermoreflectance change profiles for the GaN material along the channel width for the same range of drain voltage as the metal profiles shown in Fig. 6. Because an accurate value of the GaN C_{TH} was not obtained by the time of this writing, the profiles of Fig. 7 are presented in arbitrary units representing the magnitude of the measured thermoreflectance change on the GaN channel. The thermoreflectance signal to noise is weaker on the GaN material than on the contact metal, so the channel profiles were smoothed using a moving average of 20 pixels in the horizontal (channel width) direction.

The thermoreflectance profiles along the channel agree with the trends seen in the temperature profiles on the metal. Drain side heating increases with increasing drain voltage. Also, the formation of hotspots in the channel for extreme pinch-off bias points, $V_D = 47.5 \text{ V}$ and 50 V , match the horizontal location of the hotspots seen in the metal profiles for the same drain voltages.

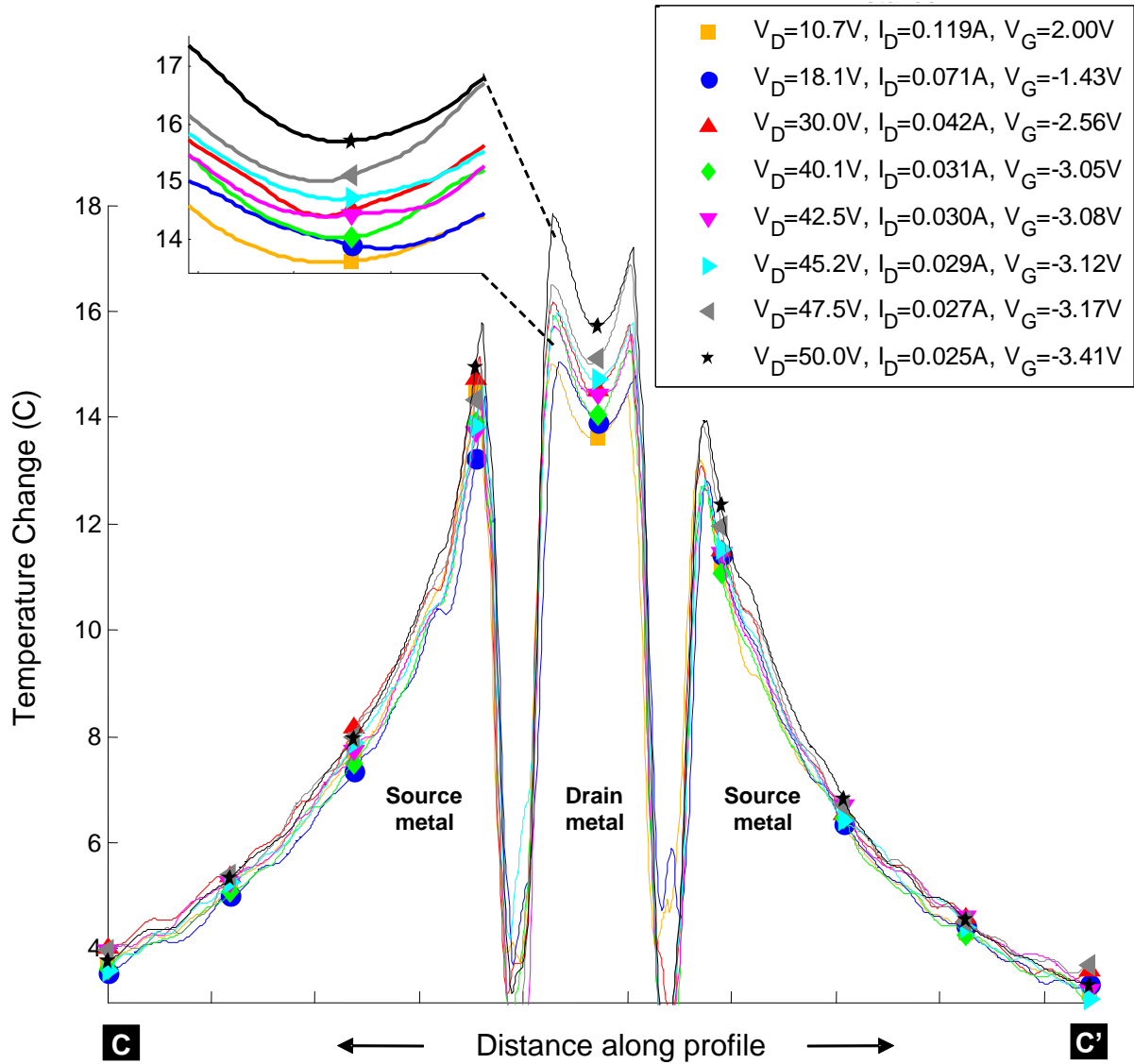


Figure 8. Vertical thermoreflectance profiles (C-C') across the HEMT. Profiles are calibrated only for the metal regions.

B. Temperature Profiles Perpendicular to Gate Width

Thermoreflectance profiles were also analyzed perpendicular to the gate width. The vertical profile line, indicated by line C-C' in Fig. 5, crosses in order: upper source contact metal, upper finger channel and gate, drain contact metal, lower finger channel and gate, and finally lower source contact metal. The vertical thermoreflectance profiles across the HEMT are plotted in Fig. 8 for the same range of drain voltage bias points ($V_D = 10.7 - 50$ V) as the horizontal profiles. The vertical profiles are temperature calibrated only for the source and drain contact metal regions. These regions are indicated in Fig. 8. The profiles reveal HEMT heating is asymmetric along the vertical axis as well as the horizontal axis. Along profile C-C' the upper source contact metal is on average 8% (1°C) hotter than the lower source metal. Similarly the drain contact metal near the upper finger is 6% hotter than

the same contact near the lower finger. Temperature distribution along the vertical profile also varied with drain voltage, and the trend was similar to the one seen for the horizontal profiles. However, this variation is more likely due to the horizontal redistribution of temperature with increasing V_D as shown in the horizontal profiles of Fig. 6. The most noticeable redistribution of temperature occurs for the highest drain voltage. For example, at $V_D = 50$ V, the maximum temperature change along the vertical profile (occurring at the drain metal near the upper gate) was ~18% greater than the temperature change at the same location for $V_D = 10.7$ V. Vertical profiles along on the right side of the HEMT (not plotted) revealed a concurrent *decrease* of ~8% in maximum temperature change on the drain metal as V_D increased from 10.7 to 50 V. This result is consistent with the hypothesis of power redistribution in the HEMT at high V_D .

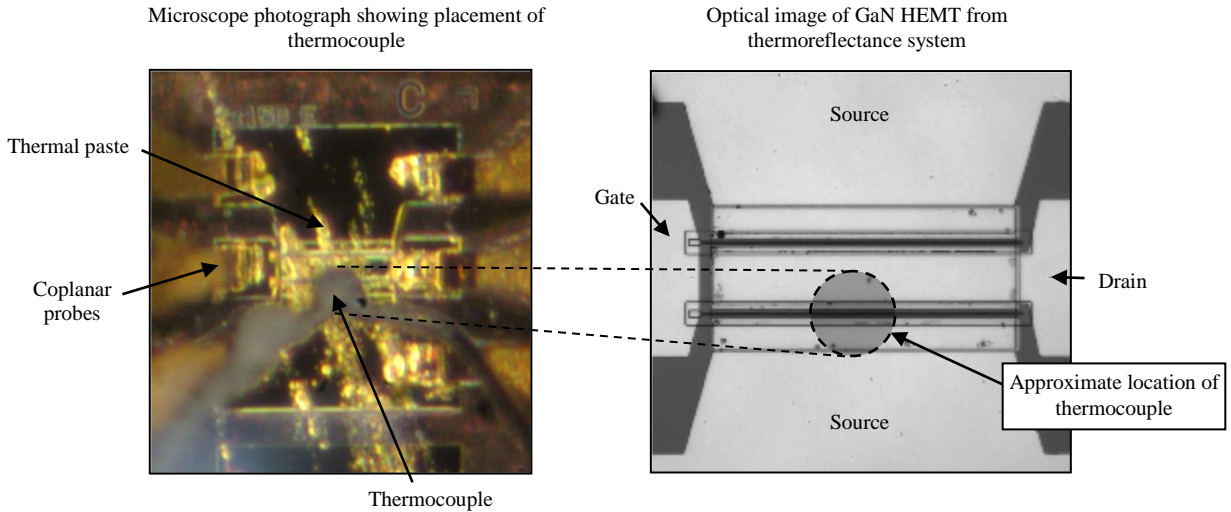


Figure 9. Microscope and CCD optical image showing HEMT and location of thermocouple measurement.

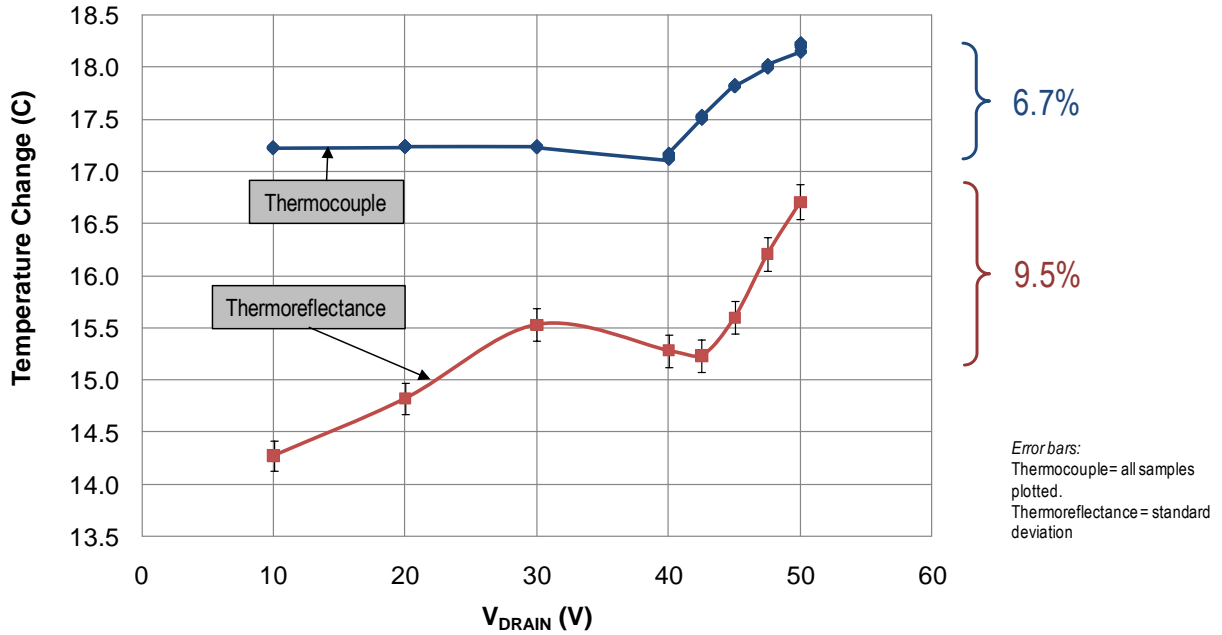


Figure 10. Comparison of single point thermocouple temperature measurements for location indicated with average thermoreflectance measurement for same area.

C. Thermocouple Measurements

Direct thermocouple measurement was used to confirm point temperature fluctuations for different HEMT pinch-off bias conditions. Although direct thermocouple measurements do not provide as much spatial temperature information as thermoreflectance images, they can be used for temperature measurement at a single location with spatial resolution approximately equal to the size of the thermocouple junction tip. For this experiment a 25 μm type E Omega thermocouple was used. The thermocouple junction tip was brought into

contact with the top surface of the GaN HEMT. Thermal paste was used to improve the thermal interface. The junction tip, approximately 50 μm in diameter, was positioned in the center of the HEMT lower finger as shown in the microscope photograph of Fig. 9. Notably, the placement of the thermocouple did not appear to affect the measurements, as seen by the electrical data. The approximate location and diameter of the thermocouple interface is indicated by the circle in the optical CCD image of the HEMT in Fig. 9. For thermocouple measurement, the HEMT was biased using constant voltage on both the gate and drain. Thermocouple

temperature was acquired using a voltmeter and LabVIEW system accurate to 50 mK.

Fig. 10 shows the thermocouple temperature on the HEMT for the same range of pinch-off bias points that were used during thermoreflectance imaging. Also plotted are the average thermoreflectance temperatures measured on the drain metal. The thermoreflectance temperatures are the average of the central third of the horizontal profile, as indicated along the line D-D' in Fig. 5. Both the thermocouple and thermoreflectance measurements show sudden fluctuation in temperature for drain voltage above $V_D = 40$ V. The thermocouple results provide additional evidence of temperature and therefore power redistribution in the HEMT at extreme pinch-off.

IV. CONCLUSION

Thermoreflectance CCD imaging was used to characterize self heating with sub-micron spatial resolution across the surface of a two finger gallium nitride high electron mobility transistor (GaN HEMT) at various stages of transistor pinch-off for equivalent device power. Two dimension temperature maps calibrated to the transistor drain and source contact metal revealed variation in temperature spatial distribution (implying non-uniform operation of the device) for the cases of greatest pinch-off and highest drain voltage.

REFERENCES

- [1] Moran, J., "The effects of temperature [0-300K] and electron radiation on the electrical properties of AlGaIn/GaN heterostructure field effect transistors" Thesis, Air Force Institute of Technology, Mar 2009.
- [2] D. Donoval, et al., "High-temperature performance of AlGaIn/GaN HFETs and MOSHFETs", *Microelectronics Reliability*, (2008)
- [3] Simms RJT, Pomeroy JW, Uren MJ, Martin T, Kuball M. Current collapse in AlGaIn/GaN transistors studied using time-resolved Raman thermography. *Applied Physics Letters*. 2008;93(20):203510.
- [4] Chowdhury U, Jimenez JL, Lee C. TEM observation of crack-and pit-shaped defects in electrically degraded GaN HEMTs. *Electron Device*. 2008;29(10):1098-1100.
- [5] Alamo J a del, Joh J. GaN HEMT reliability. *Microelectronics Reliability*. 2009;49(9-11):1200-1206.
- [6] Beechem T, Christensen A, Graham S, Green D. Micro-Raman thermometry in the presence of complex stresses in GaN devices. *Journal of Applied Physics*. 2008;103(12):124501.
- [7] Ju S, Kading OW, Leung YK, Wong SS, Goodson KE. Short-timescale thermal mapping of semiconductor devices. *IEEE Electron Device Letters*. 1997;18(5):169-171.
- [8] Tessier G, Holé S, Fournier D. Quantitative thermal imaging by synchronous thermoreflectance with optimized illumination wavelengths. *Applied Physics Letters*. 2001;78(16):2267.
- [9] D. Luerssen, J. A. Hudgings, P. M. Mayer, and R. J. Ram, *IEEE Semiconductor Thermal Measurement and Management Symposium*, 2005. p. 253-258.